A High Spatial Method to Determine Three-Dimensional Velocity Gradient Tensor using Micro Particle Image Velocimetry

Elham Tolouei[1], Warwick S. Nesbitt[2], Andreas Fouras[3], Josie Carberry[4]

1: Department of Mechanical Engineering, Monash University, Melbourne, Australia,
elham.tolouei@eng.monash.edu.au
2: The Australian Center for Blood Diseases, Monash University, Melbourne, Australia,
warwick.nesbitt@med.monash.edu.au
3: Division of Biological Engineering, Monash University, Melbourne, Australia,
andreas.fouras@eng.monash.edu.au
4: Department of Mechanical Engineering, Monash University, Melbourne, Australia,
josie.carberry@eng.monash.edu.au

Abstract Micro Particle Image Velocimetry (μPIV) is a non-invasive flow field measurement technique, which is becoming the method of choice for the investigation of micro-flows. Measurements of flows which occur within the human body represent one of the most important applications of μPIV. A three-component two-dimensional scanning micro-Particle Image Velocimetry (μPIV) technique is presented in this paper. This technique yields high spatial resolution of the wall normal velocity gradient, γ_z, which relates directly to the shear stress experienced by adhering cells. The flow characteristics around a fixed thrombus in a rectangular glass micro-slide are examined in order to understand the role of flow mechanics in platelet aggregation and thrombus formation.
Close to the wall regions of low normal velocity gradient occur around the fixed thrombus. Additionally, the in plane velocity gradient, γ_{xy}, is high around the sides of the thrombus but low at the front and rear. Accordingly a platelet moving from a relatively low shear environment at the front of the thrombus experiences increased shear at the thrombus sides followed by low shear at the rear. In-vitro observations indicate that this pattern of shear history provides favourable conditions for platelet recruitment at the rear of the thrombus.

1. Introduction

Particle Image Velocimetry (PIV) is a non-invasive flow field measurement technique, which is becoming the method of choice for many experimental fluid mechanics investigations. The fundamental mode of PIV is to record two successive images of working fluid particles illuminated by a light source such as laser. The image pairs are discretised into small interrogation areas, and correlation analysis is applied between recorded image pairs to calculate the in-plane velocity field. Over the last decade there has been an increasing interest in understanding fluid phenomena at the micro and nano length scales. The application of PIV to micro-scale measurements, micro Particle Image Velocimetry (μPIV), was introduced by Santiago *et al.* (1998) and continues to be refined.

Measurements of flows which occur within the human body represent one of the most important applications of μPIV. Platelet aggregation and thrombus formation have a critical role in arresting bleeding at site of vascular injury, but also play a pathological role in arterial diseases leading to heart attacks or strokes. The precise mechanisms by which flow properties affect thrombus formation, including platelet adhesion and aggregation, are not well understood. The function of blood elements is known to depend on hemodynamic forces, especially shear stress (Kroll 1996; Goncalves 2005; Maxwell 2006). Critical functions of blood cells, such as platelet and leukocyte adhesion relating to coagulation and immune response, occur at the vessel wall. Thus, knowledge of flow-induced shear stress at the wall is imperative to understanding these functions.

Platelets are the smallest cell in human blood and are approximately 2 to 3 μm in diameter. Monitoring platelet behaviour and the flow-induced forces they are exposed to, is particularly important in understanding how thrombi form. In order to determine the way in which the flow field affects platelet adhesion a high resolution imaging technique is required.

The complex geometry of bio-structures, such as atherosclerosis plaque, results in highly three-dimensional flow behaviour, which poses a challenge for μPIV measurement techniques. A number of methods have been developed to determine the third velocity component (out-of-plane velocity component) in μPIV experiments. Rohaly *et al.* (2001) obtained three-dimensional velocity fields in a microchannel by placing an extra off-axis rotating aperture on the microscope's light path. Yoon & Kim (2005) used three fixed off-axis apertures to perform defocused μPIV, where the diameter of the particles is proportional to out-of-plane position, enabling them to reconstruct the full three-dimensional velocity field. These methods work best for low particle density and large particle diameters of 5 μm or more. Park *et al.* (2004) used confocal laser scanning microscopy (CLSM) to measure the velocity profile in different planes in two different microtubes. Comparison of the results with conventional μPIV showed that the confocal laser scanning microscopy improves particle image contrast and the accuracy of measured velocity vector fields. However, due to low acquisition frequency and the limited light sensitivity of the optical set-up, the method is restricted to very slow flow rates (with reported Reynolds numbers in order of 10^{-3} to 10^{-2}). Park & Kihm (2006) used three-dimensional micro particle tracking velocimetry to measure the three-dimensional velocity field over a spherical object inside a microchannel. They correlated the diffraction pattern ring size variations with the defocusing distances of small particles to determine the three-dimensional particle locations and calculated the velocity vectors.

Holographic μPIV (Yang & Chuang 2005), digital holographic μPIV (Ikeda *et al.* 2005) and microscale stereoscopic PIV (Bown *et al.* 2005) have also been used to measure three-dimensional micro flows. Holographic μPIV has a complicated experimental setup and suffers from optical aberration. Stereo-μPIV is limited by the difficulty of implementing two cameras on a microscope, its cumbersome calibration procedure, and the lowered imaging accuracy due to significant optical aberration and astigmatism (Park & Kihm 2006).

An alternative for measuring the third out-of-plane velocity component and wall normal velocity gradient is the application of well-established two-dimensional μPIV techniques coupled with the concept of continuity. The advantage of this continuity based technique is that the existing two-dimensional μPIV technology is in a more advanced stage of development compared to the methods reviewed above. Bown *et al.* (2007) presented out-of-plane velocity data using a continuity based scanning μPIV method and compared them with the stereo-μPIV. They used a microchannel with backward step and calculated the out-of-plane velocity in three different planes. The minimum scanning step used by Bown *et al.* (2007) was 70 μm. The measured velocity components from the two separate methods showed good agreement.

In this paper we calculate the wall normal velocity and wall normal velocity gradients using scanning μPIV method combined with the continuity equation. The best image quality is obtained in a plane parallel to the wall of the microslide, however the normal velocity gradient at the wall is required to study platelet adhesion to the blood vessel wall. Therefore, the scanning method is well suited to determine the in-plane and out-of-plane shear rates. Previous investigations have not been able to obtain high enough resolution of the three-dimensional flow field data to study platelet adhesion. In this work we use a high spatial imaging system with a scanning step resolution of 1μm. Additionally a high image acquisition rate allows us to study higher bulk flow rates than previous

investigations. These higher flow rates are required to study physiological and pathophysiological arterial blood flows. The application of this technique to flow around a fixed thrombus will be discussed.

3. Experimental apparatus and methodology

3.1. µPIV Experimental setup

The experimental system used µPIV to measure flow fields in a micro channel. Fig. 1 shows a schematic of the experimental setup, which consisted of an epi-fluorescent upright microscope (DM RE, Leica Microsystems, Germany), a high-speed camera (MotionPro X3, Redlake Inc., FL, USA), a diode-pumped solid-state (DPSS) laser and a syringe pump (Harvard Apparatus, MA, USA). The high-speed camera was connected to the outlet port of the microscope and a 0.63× adapter in between to improve image intensity. The glass microslide was placed horizontally on the microscope and illuminated by a 200 mJ 532 nm laser, where the laser beam passes through the microscope objective. The microscope objective was a 63× water immersion lens (HCX PL APO, NA 1.2) selected to increase the amount of light gathered from the tracer particles and to maximise the signal-to-noise ratio.

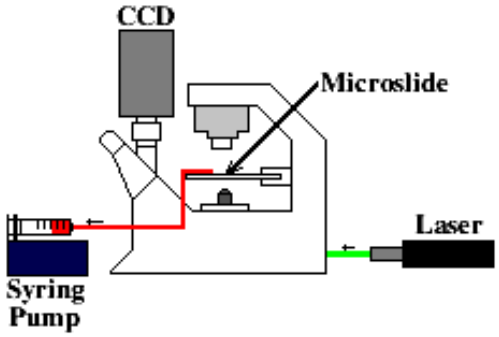

Fig 1. Schematic showing experimentals setup

The experiment was carried out in a rectangular glass microslide, cross-section 2mm × 0.2mm and 100mm long (Vitrotubes, VITRO COM, Mountain Lakes, NJ, USA). As shown in Fig. 2, the reference axes are indicated by x, y and z, with corresponding velocity components u, v and w, where the direction of the upstream flow is parallel to the unit vector x.

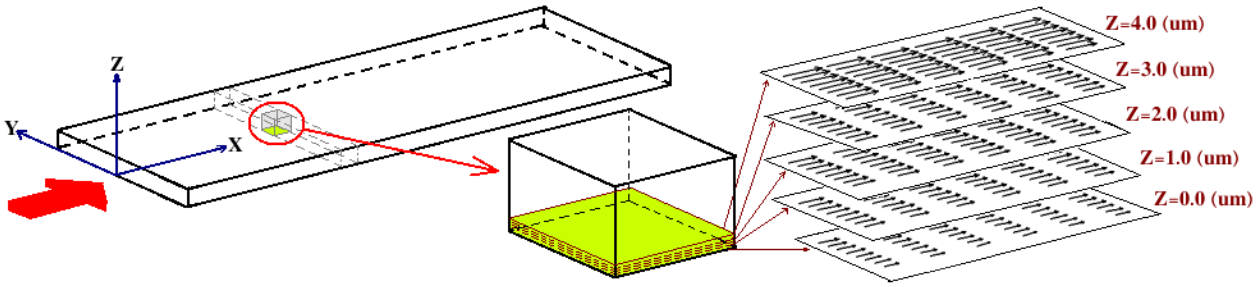

Fig 2. Schematic diagram illustrating the scanning method. The figure shows the coordinate system, the volume illumination and the PIV measurement planes. The microscope objective is located under the microslide

3.2. Sample preparation: thrombus and working fluid samples

The fixed thrombus was prepared by coating a section of the microslide with collagen (10 µg/ml) to promote platelet adhesion on glass. The microslide was then washed out with Tyrode's buffer. Whole blood (anticoagulated with Hirudin) obtained from healthy human donors was then perfused through the coated-microslide at the constant flow rate of 1.44 ml min^{-1}, which corresponds to a wall shear rate of 1800 s^{-1}, to form the thrombus. Once the thrombus has reached a suitable height

the blood flow was stopped and the thrombus was fixed.

In order to perform μPIV, physiological saline, seeded with 1% w/v 1.0 μm diameter red fluorescent particles (R0100, Duke Scientific, CA, USA), was selected as the working fluid. The fluorescent particles stream in the middle section of microslides resulting in insufficient particles near the walls. In order to overcome the low density of fluorescent particles near the wall, 10% washed red blood cells were added to the working fluid. Although the red blood cells affect the velocity profile their effect on near wall velocity profile (up to 4 micron height) is negligible. 2% Bovine serum albumin (BSA) was added to prevent clumping of the fluorescent particles. The flow rate of working fluid inside the microslide was kept constant at 0.44 ml min^{-1}. If an idealised poiseuille flow profile is assumed this flow rate corresponds to a theoretical wall shear rate of $\gamma_{z,th} = 550\ s^{-1}$.

3.3. Experimental technique

The in-plane velocity field around the fixed thrombus was measured using μPIV. In order to calculate the out-of-plane velocity a scanning method was used. The in-plane velocity field was calculated at five different z positions from the bottom wall (z=0.0) to z=4.0 μm with scanning step 1μm as shown in Fig. 2.

The flow field images were recorded by the high-speed camera at 1000 Hz and at a resolution of 3.4 pixels/μm. The velocity field was calculated from consecutive image pairs using an in-house PIV software (Fouras *et al.* 2007). The software employs an ensemble averaging cross-correlation technique between image pairs on each interrogation area and statistically, the maximum value of the cross-correlation is the most likely particle displacement within the interrogation region. A final interrogation window size of 8×8 with an overlap ratio of 0.5 was used.

The in-plane velocity fields at different z positions were used to calculate the full three component velocity fields. The in-plane velocity gradients, $\frac{\partial u}{\partial x}, \frac{\partial u}{\partial y}, \frac{\partial v}{\partial x}$, and $\frac{\partial v}{\partial y}$ were first determined from the in-plane velocity data at each points of the three-dimensional grid. A second order five points polynomial curve fitting method was used to determine these in-plane derivatives. The out-of-plane velocity gradients, $\frac{\partial u}{\partial z}$ and $\frac{\partial v}{\partial z}$, were calculated using second order polynomial curve fitting between all experimental planes. Then the continuity equation, $\nabla\vec{V}=0$, was solved for the whole domain to calculate the first out-of-plane velocity gradient, $\frac{\partial w}{\partial z}$. With the out-of-plane velocity gradient and no-slip boundary condition at the wall the out-of-plane velocity, w, can be calculated. Finally the last two velocity gradients, $\frac{\partial w}{\partial x}, \frac{\partial w}{\partial y}$, were computed at each point.

4. Results and Discussion

The main improvement offered by the new technique is improved resolution and ability to measure physiological flows. The velocity measurement is performed in parallel planes with in-plane spatial resolution of 0.294 (μm/px). The resulting three-dimensional flow field obtained around a thrombus is able to reveal mechanisms of platelets adhesion and thrombi formation *in vitro*.

4.1. Plain microslide without obstacle

To evaluate the performance of the scanning μPIV technique near the wall the case of flow over a plain microslide was examined. Fig. 3 shows the average velocity in each z-plane obtained by averaging 500 image pairs, where the vertical error bars are one standard deviation. The experimental results were compared with Poiseuille flow for steady flow through a long, straight rigid rectangular channel. The equation used to calculate the analytical velocity profile of the rectangular channel with y and z cross section is:

$$u_x(y,z) = \frac{48Q}{4\pi^3 hw} \times \frac{1}{1 - \frac{192w}{\pi^5 h} \sum_{i=1,3,5,\cdots}^{\infty} \frac{1}{i^5} \tanh\left(\frac{i\pi h}{2w}\right)} \times \sum_{i=1,3,5,\cdots}^{\infty} \frac{(-1)^{\frac{i-1}{2}}}{i^3} \left[1 - \frac{\cosh\left(\frac{i\pi z}{2w}\right)}{\cosh\left(\frac{i\pi h}{2w}\right)}\right] \cos\left(\frac{i\pi y}{2w}\right) \quad (1)$$

where u_x is the fluid velocity in the x-direction, w and h are the width and height of the microslide, respectively, and Q is the bulk flow rate.

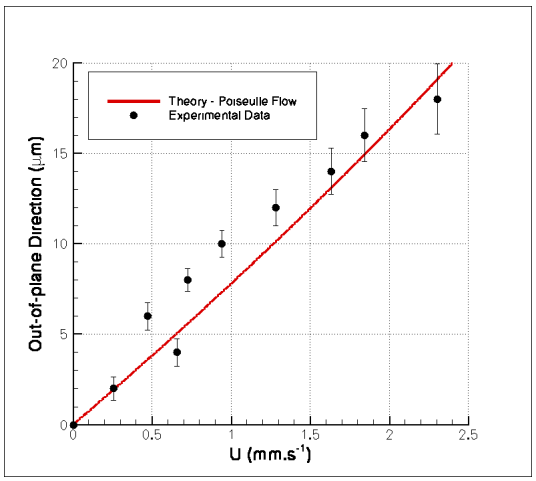

Fig. 3 Out of plane velocity profile obtained with experimental data (dots) compared with the theoretical profile (solid line) at a bulk shear rate of $\gamma_{z,th}$ =150 s^{-1}.

Generally, the experimental results are in reasonable agreement with the analytical solution. Due to low particle density and high out-of-focus effects, the measured velocity is typically over-estimated by μPIV techniques. Furthermore, errors are introduced due to the difficulty of determining the exact location of the wall. However, as the velocity profile is approximately linear near the wall not knowing the exact location of the wall does not prevent accurate calculation of the wall normal velocity gradient. Due to the defocusing phenomenon in planes away from the focal plane, the standard deviation of velocity in planes above z = 10 μm is greater than the standard deviation of velocity below z = 10 μm.

The normal and in-plane velocity gradients in the plain rectangular glass microslide with the measurement focal plane at z = 8μm are shown in Figures 4 and 5, respectively. The gradients were measured with 10 scanning planes between the wall, z = 0μm, and z = 18μm. As expected both the normal and in-plane velocity gradients are uniform except for some errors near the boundary. The results compare well with the theoretical value of $\gamma_{z,th}$ = 150 for the normal velocity gradient and the fact that the in-plane gradient should be approximately zero.

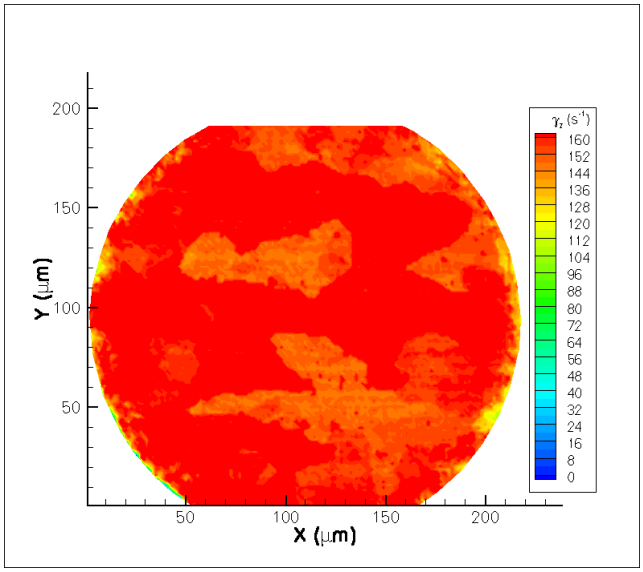

Fig. 4 Normal velocity gradient in a plain glass microslide, $\gamma_{z,th}$ =150 s^{-1}, z=8 μm.

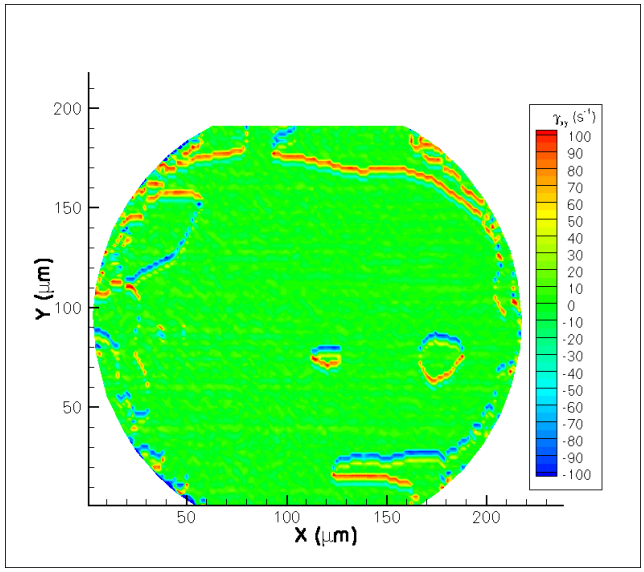

Fig. 5 In-plane velocity gradient in a plain glass microslide, $\gamma_{z,th}$=150 s^{-1}, z=8 μm.

4.2. Fixed thrombus in a microslide

The velocity gradients and normal velocity fields around a fixed thrombus are shown in Figures 6 through 8. The data were acquired at a wall shear rate of $\gamma_{z,th}$ = 550 s^{-1} and the flow is from left to right. Velocity vector fields were resolved in multiple planes using the μPIV technique. The velocity vectors field layers were interrogated using an 8×8 pixel interrogation region size with a 50% overlap. As shown in Fig. 6, far from the thrombus the normal velocity gradient is uniform and similar in magnitude to the theoretical value. Around the large central thrombus the flow pattern is considerably altered. The normal velocity gradient is roughly zero next to the central thrombus, increasing gradually to approximately 580 s^{-1} 70-80 μm from the thrombus. The non-uniformity of the velocity gradient away from the thrombus, evident in Fig. 6(b), may be attributed to the present of the red blood cells in the working fluid.

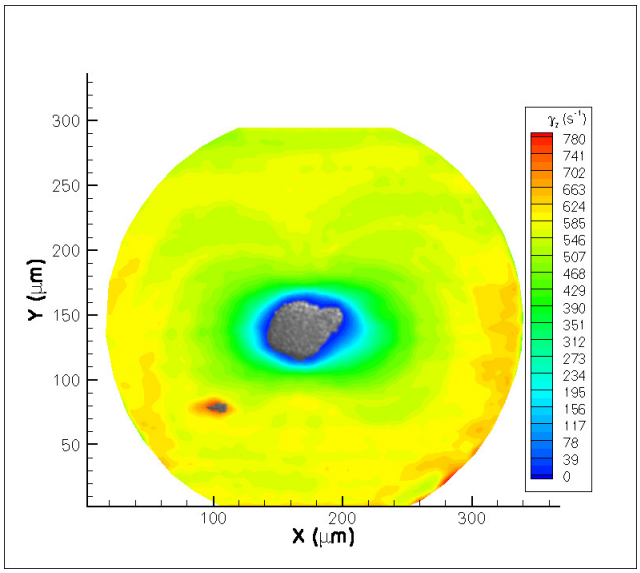

Fig. 6(a) Distribution of normal velocity gradient around a fixed thrombus, $\gamma_{z,th}$ =550 s^{-1}, z=2 μm.

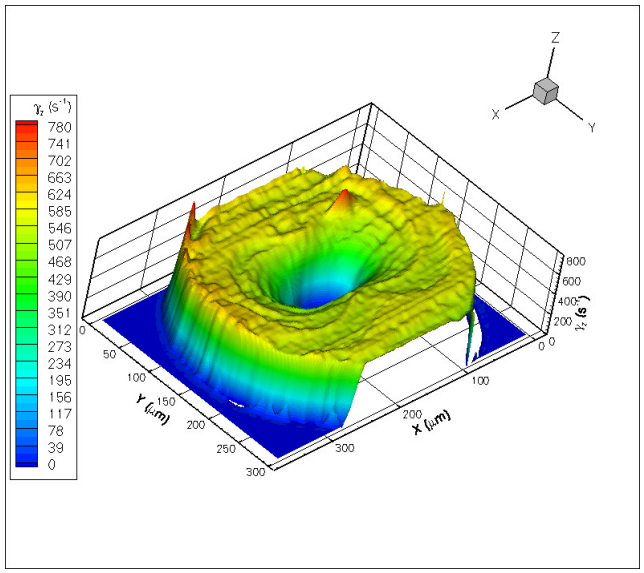

Fig. 6(b) Three-dimensional distribution of normal velocity gradient around a fixed thrombus, $\gamma_{z,th}$ =550 s^{-1}, z=2 μm.

The in-plane velocity gradient and velocity vector field at z = 2 µm are presented in Fig. 7. The maximum in-plane velocity gradient occurs around the sides of the thrombus at the top and bottom apexes. These locations correspond to rapid turning of the flow and changes in the magnitude of the v velocity component. It has been shown (Nesbitt *et al.* 2008) that further thrombus growth occurs downstream of the existing thrombus. Preliminary observations indicate that this may be linked to the high in-plane velocity gradient around the sides of the thrombus which prevent further platelet adhesion in these regions.

The normal velocity around the thrombus is plotted in Fig. 8. The maximum normal velocity occurs upstream of the thrombus as a portion of the flow in the z = 2 µm plane is displaced upwards by the presence of the thrombus. Similarly there is downwards motion of the flow some distance behind the thrombus. The height of the central thrombus is significantly greater than the data planes studied. Therefore, the majority of the flow immediately around the thrombus is expected to be in plane; this was confirmed by the relatively small values of w plotted in Fig. (8). In the lower left portion of the Fig 6(a) flow passes over a small flat thrombus and a local increase in the normal velocity gradient is evident, corresponding changes in w are observed in Fig. 8.

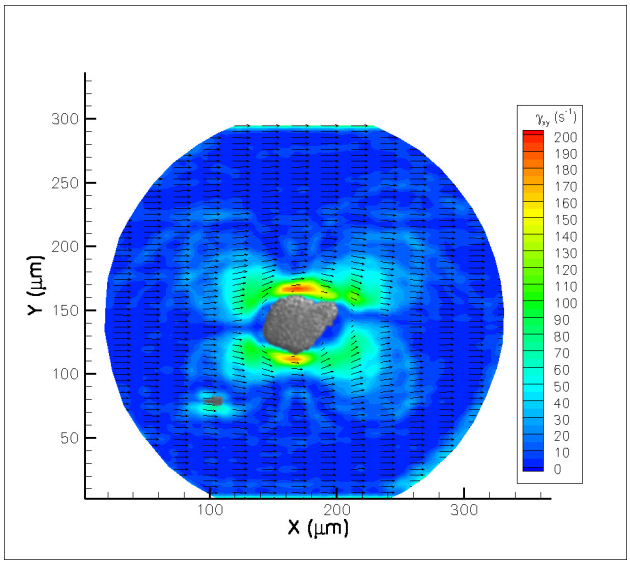

Fig. 7 Two-dimensional velocity vector field and in-plane velocity gradient distribution around a fixed thrombus, $\gamma_{z,th}$ =550 s^{-1}, z=2 µm.

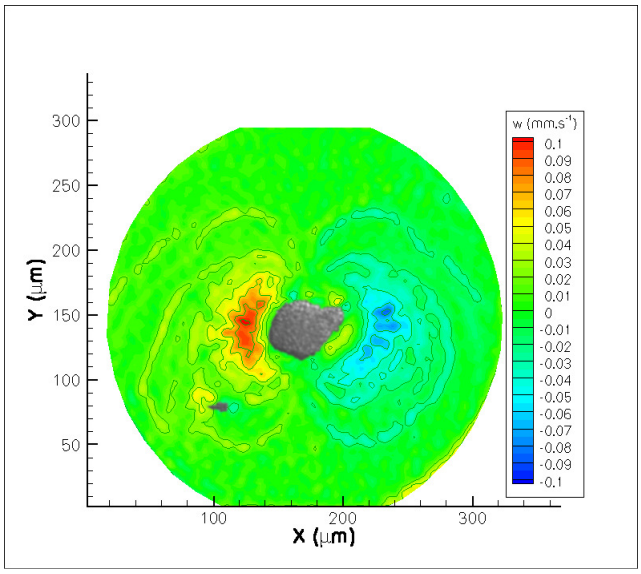

Fig. 8 Contours of normal velocity around a fixed thrombus, $\gamma_{z,th}$ =550 s^{-1}, z=2 µm. Note in this plane u ≈ 1.1 mm.s^{-1}

5. Conclusions

This study provides an insight into how advanced experimental fluid dynamics may be utilized to analyze flows for biological applications. The method of scanning µPIV has been used to examine near wall flow conditions in a glass microslide around a fixed thrombus. Conventional two-dimensional two-component µPIV data has been obtained on a number of parallel planes near the microslide wall to measure the in plane velocity gradients and combined with continuity equation to calculate the out-of-plane velocity gradients. The accuracy of the measurements was limited by the difficulty in obtaining accurate measurement close to the wall. A number of techniques are being investigated to overcome this.

Investigation of flow fields and velocity gradients around the fixed thrombus revealed a region of low normal velocity gradient immediately around the thrombus, corresponding to an environment

where platelets experience low normal shearing stresses. The normal velocity gradient increases gradually to the bulk velocity gradient at a distance of 70-80 microns from the thrombus. The in plane velocity gradient is maximum around the sides of the thrombus but low at the front and rear. The maximum in-plane velocity gradient is still significantly smaller than the normal velocity gradient in the bulk flow. This illustrates the importance of measuring wall normal velocity gradients.

Platelet recruitment around an existing thrombus generally occurs at the rear of the thrombus, corresponding to the region where both the normal and in-plane velocity gradients are low. Importantly, the platelets experience a high in plane velocity gradients as they move around the side of the thrombus before reaching the lower shear environment at the rear of the thrombus. Additionally, the velocity behind the thrombus is relatively low and a small negative w velocity component may act to push the platelets towards the wall. These factors provide favourable conditions for further platelet adhesion and aggregation in the region behind the thrombus.

6. References

Bown MR, Macinnes JM, Allen RWK (2007) Three-component micro-piv using the continuity equation and a comparison of the performance with that of stereoscopic measurements. Exp Fluids (N 0723-4864): 197-205

Bown MR, MacInnes JM, Allen RWK, Zimmermann WBJ (2005) Three-component micron resolution velocity measurements using stereoscopic micro-piv. In: The 6th international symposium on particle image velocimetry, Pasadena, California, USA, September 2005.

Fouras A, Lo Jacono D, Hourigan K (2007) Target-free stereopiv: A novel technique with inherent error estimation and improved accuracy. Exp Fluids. DOI: 10.1007/s00348-007-0404-1.

Goncalves I, Nesbitt WS, Yuan YP, Jackson SP (2005) Importance of temporal flow gradients and integrin alpha (IIb) beta(3) mechanotransduction for shear activation of platelets. Journal of Biological Chemistry 280(15): 15430-15437.

Ikeda K, Ooms T, Westerweel J (2005) Feasibility study on microscopic digital holographic piv. In: The PIVNET2 international workshop on microPIV and applications in microsystems.

Kroll MH, Hellums JD, Mcintire LV, Schafer AI, Moake JL (1996) Platelets and shear stress. Blood 88(5): 1525-1541.

Maxwell MJ, Dopheide SM, Turner SJ, Jackson SP (2006) Shear induces a unique series of morphological changes in translocating platelets-effects of morphology on translocation dynamics. Arterioscler. Thromb. Vasc. Biol. 26(3): 663-669.

Meinhart CD, Wereley ST, Santiago JG (1999) PIV measurements of a microchannel flow. Exp Fluids 27(5): 414-419

Nesbitt WS, Westein E, Tolouei E, Fu J, Fras A, Carberry J, Jackson SP (2008) Discovery of a new mechanism driving thrombus growth. Under Review for publication in Nature Medicine

Park JS, Choi CK, Kihm KD (2004) Nanoparticle tracking using CLMS and OSSM imaging. Journal of Heat Transfer.

Park JS, Kihm KD (2006) Three-dimensional micro-PTV using deconvolution microscopy. Exp Fluids. 40(N 0723-4864): 491-499.

Rohaly J, Lammerding J, Frigerio F, Hart DP (2001) Monocular 3d active micro-ptv. In: The 4th international symposium on particle image velocimetry, Gottingen, Germany, September 2001.

Santiago JG, Wereley ST, Meinhart CD, Beebe DJ, Adrian RJ (1998) A particle image velocimetry system for microfluidics. Exp Fluids. 25(4): 316-319.

Yang CT, Chuang HS (2005) Measurement of a microchamber flow by using a hybrid multiplexing holographic velocimetry. Exp Fluids. 39(N 0723-4864): 385-396.

Yoon SY, Kim KC (2005) Three dimensional particle tracking and velocity measurement in a microchannel by using an aperture with three holes. In: The 6th international symposium on particle image velocimetry, Pasadena, California, USA, September 2005.